

RUGGED CERAMIC WINDOW FOR RF APPLICATIONS*

Michael Neubauer[#], Rolland P. Johnson, Muons, Inc., Batavia, IL USA
 Robert Rimmer, Tom Elliot, Mircea Stirbet, JLab, Newport News, VA USA

Abstract

High-current RF cavities that are needed for many accelerator applications are often limited by the power transmission capability of the pressure barriers (windows) that separate the cavity from the power source. Most efforts to improve RF window design have focused on alumina ceramic, the most popular historical choice, and have not taken advantage of new materials. Alternative window materials have been investigated using a novel *Merit Factor* comparison and likely candidates have been tested for the material properties which will enable construction in the self-matched window configuration. Window assemblies have also been modeled and fabricated using compressed window techniques which have proven to increase the power handling capability of waveguide windows. Candidate materials have been chosen to be used in fabricating a window for high power testing at Thomas Jefferson National Accelerator Facility.

INTRODUCTION

Recent work at Thomas Jefferson National Laboratory (JLab) has shown that a single, rugged waveguide window may work very well for high-power CW RF coupler applications [1,2]. JLab is currently in the process of developing a 1.5 GHz waveguide window as part of the development of a high-current cryomodule for Energy Recovery Linac (ERL) and Free Electron Laser (FEL) applications [3]. The average-power handling requirements for these windows are significantly greater than those anticipated for the International Linear Collider (ILC). Currently, the complicated ILC couplers (TTF-III) can handle peak powers on the order of a megawatt, but the average power handling capability is limited to tens of kilowatts [4,5,6].

The fundamental features of the window design concept championed here include the self-matching nature of the iris depth and ceramic thickness [7], and a ceramic window that is entirely contained within the aperture of the rectangular waveguide. A key feature that allows the increased power handling capability of this window design is the pre-stressing of the ceramic window to place it into a compressed state so that the tensile stresses that result from RF heating are almost completely eliminated.

The development of the high average-power waveguide windows at JLab have been based on this design concept, which has led to very reliable and cost effective solutions. The concept has been used successfully for the SLAC B-factory and Spear-3 light source at lower frequencies [8] and a similar 700 MHz design, was developed for LEDA at LANL [9] and was tested to almost 1 MW CW.

* Supported in part by USDOE SBIR Grant DE-FG02-08ER85171
 mike@muonsinc.com

MATERIAL CHARACTERIZATION

In order to make choices among various ceramics for microwave windows based upon thermal considerations, it appears that the ratio of thermal conductivity to loss tangent may be a reasonable approach. The argument goes: that for every watt generated by the losses in the ceramic as a function of the loss tangent ($\tan \delta$), the temperature differential required to remove that watt is determined by the thermal conductivity (k) of the material.

This means if the ratio: “Merit Factor” = $k/\tan \delta$ remains constant at low temperatures, then the reduction in $\tan \delta$ will have no impact on the thermal stresses in the window because the temperature profile from the center to the edge will remain constant. It may also suggest we can make meaningful judgments about the relative merits of various ceramics.

Table 1 summarizes the calculation of the *Merit Factor* using published data from various sources. If there were ranges of data from various sources, simple averages were used for $\tan \delta$ and k , and where necessary, the data was scaled in frequency ($\tan \delta \propto f$) so that the *Merit Factor* shown is for 1 GHz at room temperature.

Table 1: Merit Factor for Various Materials

Room Temperature Data (approx 1 GHz)			
Material	Loss Tangent $\tan \delta$	Thermal Conductivity W/m/K	Quality Factor $\times 10^6$
AL ₂ O ₃	0.00018	31.5	0.179
BeO	0.00110	251.5	0.229
BN	0.00025	61.0	0.244
SiC	0.00360	129.8	0.036
SiN	0.00360	26.3	0.007
AlN	0.00195	154.0	0.079
Sapphire	0.00001	38.0	3.800
Transtar	0.00010	35.0	0.350
Shapal-M	0.00700	90.0	0.013
ALON	0.00031	9.5	0.031

COMPRESSION RING DESIGN

The compression ring design has three main requirements:

- 1) The finished window must be left in a pre-stressed condition with radial forces only.
- 2) During cool-down and radial compression, axial forces that can put the window edge under damaging axial tensile stress must be relieved by a copper buffer layer.
- 3) The compression ring must contain a channel for liquid coolant.

Construction of the buffer layer is typically done by plating large amounts of copper on the stainless steel ring. This is time consuming and costly. A better way was investigated in this Phase I program. A copper ring was brazed into the inside diameter of the stainless steel ring. This braze is not trivial and requires significant process controls to minimize braze gaps between the copper and stainless steel which can lead to hot spots in the final assembly. In addition, the copper buffer layer is designed to be .020 thick, and post machining the assembly may lead to removing too much copper so that the buffer layer may not be effective. Figure 1 shows an example of a perfect buffer layer.

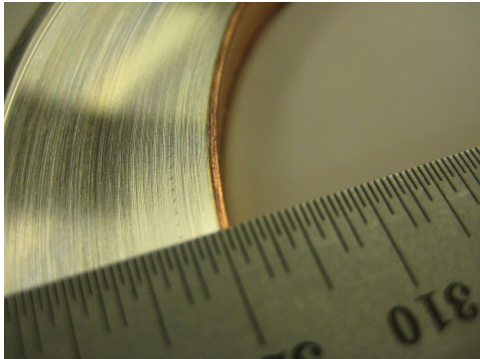


Figure 1: The perfect buffer layer.

The process technique for making the buffer layer is critical to the construction of rugged ceramic windows. During the braze of a completed window, the stainless steel compression ring goes through a critical extrusion process. The extrusion results in a ring that is smaller in diameter at room temperature, than it started out and it is this reduction in diameter that makes the pre-stressed window. Modeling the extrusion process is a critical first step in calculating the amount of pre-stress in the completed window. The ANSYS model of the extrusion process is shown in Fig. 2.

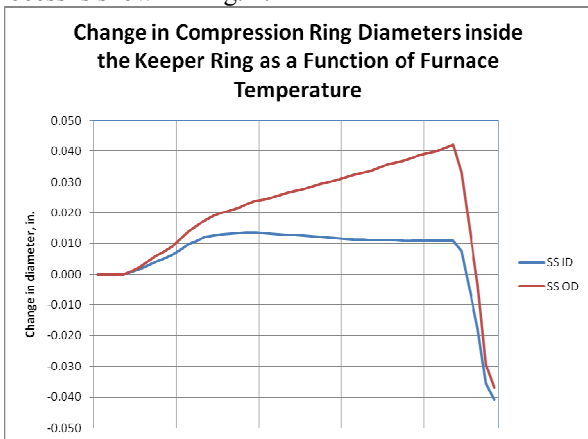


Figure 2: ANSYS model of the extrusion process with a starting gap between the compression ring outside diameter and molybdenum keeper ring inside diameter of .006 in. The red curve is the outside diameter of the compression ring, and the blue curve is the inside diameter of the compression ring.

From 25C to 200C, the outside diameter of the stainless

steel compression ring grows at the rate of the thermal expansion of stainless steel as shown by the slope of the curve. At 200C, the stainless steel compression ring has touched the molybdenum keeper ring inside diameter, and must now grow at the rate of thermal expansion of the molybdenum as shown by the reduced slope of the curve. Because the outside of the stainless steel is restrained by the molybdenum keeper ring, the inside diameter of the stainless steel compression ring gets smaller. The stresses inside the stainless steel exceed its yield strength at the elevated temperatures, so that at cool down from 1000C to room temperature, the diameter of compression ring is smaller than it was at the beginning of this process.

The ANSYS model of this process compares well with those measured in actual rings. All measurements of the actual rings had the ID changing more than the OD with numbers comparable to those calculated.

MODELING THE BRAZING PROCESS

During brazing the critical starting variables are the gaps between the ceramic window and stainless steel compression ring and the gap between the stainless steel compression ring and the keeper ring. These gaps determine the final stresses in both the compression ring and the window after brazing and cooling down. As shown in Table 2, the object is to have no stress on the window compression ring will be further extruded with a larger ID and less pressure will be exerted on the window

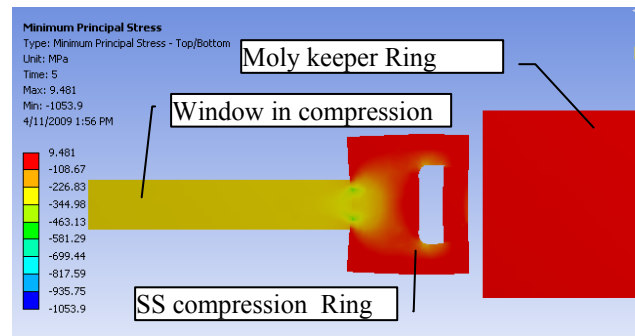


Figure 3: Axi-symmetric ANSYS calculations of the braze cycle showing the deformation of the stainless steel compression ring after cool down and the minimum principal stress (compression). The window is uniformly compressed.

Table 2: ANSYS calculations of the final compression on the window as a function of starting gap between the window and the stainless steel compression ring. The gap between the compression ring and the molybdenum keeper ring is fixed at .006 in.

Compression on the Window		
The gap between the keeper ring and the compression ring before braze = .006 in	Gap Between Window and Compression Ring Before Brazing	
	.010 in	.006 in
Compression at Braze Temp	0 psi	4844 psi
Final Compression	26780 psi	26608 psi

at room temperature. In addition, if the gap at braze temperature is not correct, the braze material will not flow properly throughout the joint. Figure 3 shows the ANSYS calculation with deformed stainless steel compression ring placing the window in compression.

MODELING THE EFFECT OF PRE-STRESS

The amount of pre-stress in a disk window determines the allowable temperature difference between the center of the window and the outer edge, as shown in Table 3.

Table 3: ANSYS calculations of the edge tensile stress in alumina and the projected increase in power handling capability as a result of pre-stressing.

uniform heating	Temperature		Edge Stress	Tensile		% of limit	
	total	center		edge	MPa	psi	w/o pre-stress
0.05	16	48	22	33	4785	32%	-147%
0.07	22	58.33	22	46.45	6735	45%	-134%
0.1	31	73	22	66	9570	64%	-115%
0.2	62	125.8	22	132.72	19244	128%	-50%
0.25	78	151	22	165	23925	160%	-19%
0.3	93	178	22	199	28855	192%	14%
0.35	109	204	22	232	33640	224%	46%

COLD TESTING WINDOW MATERIALS

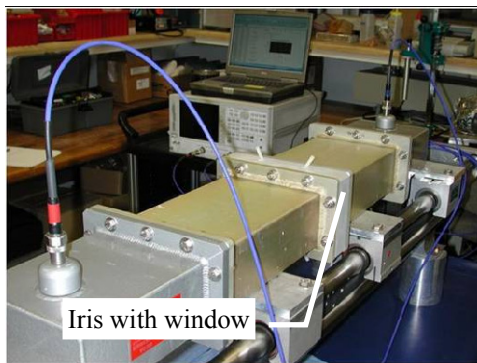


Figure 4: Windows samples of sapphire, aluminum nitride, and Transtar® are tested in the iris.

Samples of window materials were tested in a cold test fixture (shown in Fig. 4) to determine the resonant frequency in the iris designed for 1497 MHz. In the self-matching window design, the dielectric constant determines the thickness of the window for precise determination of the matching frequency. However, it is not always easy to predetermine that thickness because of the fluctuations in the manufacturing of the ceramic materials, so cold tests are the beginning of that the process as shown in Fig. 5. The Δ Freq is therefore the error in knowing the dielectric constant of the sample.

Sample	Thickness (in)	Resonant Frequency (MHz)	Δ Freq from 1497 (MHz)	S21 (db)
Sapphire #1	0.298	1512.125	15.125	0.02
Sapphire #2	0.297	1513.250	16.250	0.019
Aluminum Nitride #1	0.331	1489.312	-7.688	0.224
Aluminum Nitride #2	0.331	1493.600	-3.400	0.222
Transtar #1	0.290	1525.061	28.061	0.171
Transtar #2	0.289	1523.438	26.438	0.126

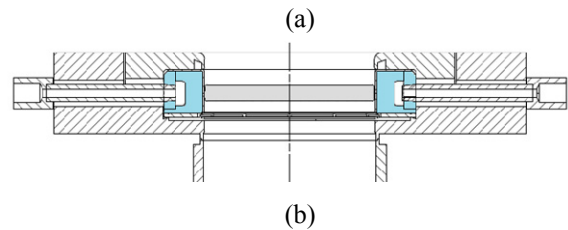


Figure 5: (a) Cold test measurements of the window in the iris. (b) Schematic view of the window in the iris with the narrow wall of WR650.

REFERENCES

- [1] "The JLab Ampere-Class cryomodule", R. Rimmer et. al., Proc SRF 2005, Cornell University, July 11-15, 2005.
- [2] "JLab High-Current CW Cryomodules for ERL and FEL Applications", R. Rimmer et. al., Proc. PAC07, Albuquerque, New Mexico, June 25-29, 2007.
- [3] "High-Power Windows for WR650 Waveguide Couplers", M. Stirbet et. al., Proc. PAC07, Albuquerque, New Mexico, June 25-29, 2007.
- [4] "TTF3 Power Coupler for the ILC – Fabrication, tests and Performance," Wolf-Dietrich Möller, 2005 ILC Meeting, Snowmass.
- [5] "Status and Operating Experience of the TTF Coupler", D. Kostin and W.-D. Möller, Proceedings of LINAC 2004, Lübeck, Germany, pp 156-8.
- [6] "Power Couplers of the ILC", T. Treado and S. Einarson, Proc. PAC07, Albuquerque, New Mexico, June 25-29, 2007.
- [7] "High-Power RF Window Design for the PEP-II B Factory", M. Neubauer et. al., Proc. EPAC94, London, England, June 27 - July 1, 1994. SLAC-PUB-6553.
- [8] "High-Power RF Window and Coupler Development for the PEP-II B Factory", M. Neubauer et. al., Proc. PAC95, Dallas, Texas, May 1-5 1995, pp 1803-5. SLAC-PUB-95-6897, LBL 37250.
- [9] "A High-Power L-Band RF Window", R.A. Rimmer et. al., Proc. PAC 2001, Chicago., LBNL-47968, LAUR 01-2574.